Mapping Insect-Induced Pine Mortality in the Daniel Boone National Forest, Kentucky Using Landsat TM and ETM+ Data

John K. Maingi
Department of Geography, Miami University, Oxford, Ohio 45056

William M. Luhn
Daniel Boone National Forest, USDA Forest Service, 1700 Bypass Road, Winchester, Kentucky 40391

Abstract: A decision tree classifier was used to create a three-species conifer map of the Daniel Boone National Forest, Kentucky using Landsat TM images and ancillary data. The resulting map had an overall classification accuracy of approximately 82%. In the second part of the study, Landsat TM and ETM+ images acquired in 1995 and 2002, respectively, were used to evaluate five change-detection techniques for mapping conifer damage caused by southern pine beetle (SPB). PCA and SARVI2 change-detection techniques resulted in the highest classification accuracies. Over 60% of the conifer species were killed as a result of SPB infestation.

INTRODUCTION

The southern pine beetle (SPB; *Dendroctonus frontalis* Zimm.) is one of the largest single cause of natural disturbance in forests of the southeastern United States. The value of timber and pulpwood lost to SPB can reach $237 million per year (Price et al., 1998). The beetles most commonly mass-attack the trunks of mature pine trees, but may attack and kill young pines. The beetle prefers loblolly (*Pinus taeda* L.) and shortleaf (*Pinus echinata* Mill.) pines, but will also successfully attack and kill Virginia (*Pinus virginiana* Mill.), pond (*Pinus serotina* Michx.), table-mountain (*Pinus pungens* Lam.), longleaf (*Pinus palustris* Mill.), slash (*Pinus elliottii* Engelm.), and pitch (*Pinus rigida* Mill.) pines. Beetle populations remain at endemic levels for years until populations attain epidemic levels for a two- or three-year period. The cycles occur about every 7–10 years (Day, 1997).

In 2000, SPB populations rapidly expanded to cover federal, state, and private lands in portions of Alabama, Florida, Georgia, Kentucky, Mississippi, North Carolina, South Carolina, Tennessee, and Virginia. The mild winter and extended drought exacerbated the situation by providing optimum habitat for SPB. The 1999–2002 SPB outbreak was widespread in the southeastern forests, devastating many of the pine ecosystems. In the Daniel Boone National Forest (DBNF), Kentucky, for example, the pine/pine-hardwood habitat for the red cockaded woodpecker (*Picoides borealis*), a

GIScience & Remote Sensing, 2005, **42**, No. 3, pp. 224-250.

federally listed endangered species, was so devastated that the remaining known populations of the species had to be relocated to the Carolina Sandhills National Wildlife Refuge, South Carolina, and the Ouachita National Forest, Arkansas.

Early detection of new infestations is the first step in controlling SPB and in reducing timber losses. Aerial detection of SPB damage is accomplished by conducting periodic flights over pine forests in small fixed-wing aircraft and plotting suspected SPB spots (groups of dead and dying pine trees) on maps or aerial photographs. Once detected from the air, suspected spots are visited on the ground to confirm the causal agent and assess the need and priority for control (Billings and Pase, 1983). These techniques can be subjective and labor intensive. Automated change detection using satellite data could allow for timely and consistent estimates of defoliation trends over large areas and make it easier to capture this information into a Geographic Information System (Muchoney and Haack, 1994).

The current study seeks to understand the magnitude of the latest SPB epidemic within the Daniel Boone National Forest (Fig. 1) and utilizes pre- and peak- SPB outbreak Landsat TM and ETM+ images acquired in 1995 and 2002, respectively. It was necessary to create a conifer species map for 1995 in order to isolate land-cover changes between 1995 and 2002 within and among conifer species. There is currently no information on stand composition and characteristics outside federally administered lands within the DBNF, and therefore the conifer map created is a useful beginning to bridging this information gap. Results from this project will make it possible to identify the remaining stands of healthy pine, and areas where restoration efforts should be concentrated. The maps should also be useful to guide timber salvage operations and guide the removal of accumulated forest fuels to reduce fire danger. In addition, a SPB mortality map is an essential ingredient in modeling SPB outbreak risk.

Goal and Objectives

The goal of this research was to determine the extent and magnitude of SPB-induced forest damage at the DBNF. This goal was achieved using pre- and peak-SPB outbreak Landsat TM and ETM+ images acquired in 1995 and 2002, respectively, and change-detection techniques. Derived land-cover change maps (across all land cover types) were used together with a conifer species map to extract only those changes affecting conifer species. The specific objectives of this research are to: (1) create a conifer species map of the DBNF before SPB outbreak, utilizing a 1995 Landsat TM image, image enhancements, and ancillary data; and (2) evaluate the suitability of five change-detection techniques in mapping conifer species change resulting from SPB infestation between 1995 and 2002, utilizing Landsat TM and ETM+ images.

This research was conducted in two parts. In the first part, a conifer species map was created, and in the second the suitability of five change-detection techniques was evaluated in mapping SPB-induced forest damage. The methods and results for the two parts will be presented separately.

Remote Sensing and Forest Damage Assessment

Remotely sensed data and various change detection techniques have been used to detect and assess forest damage. Nelson (1983) evaluated the utility of image

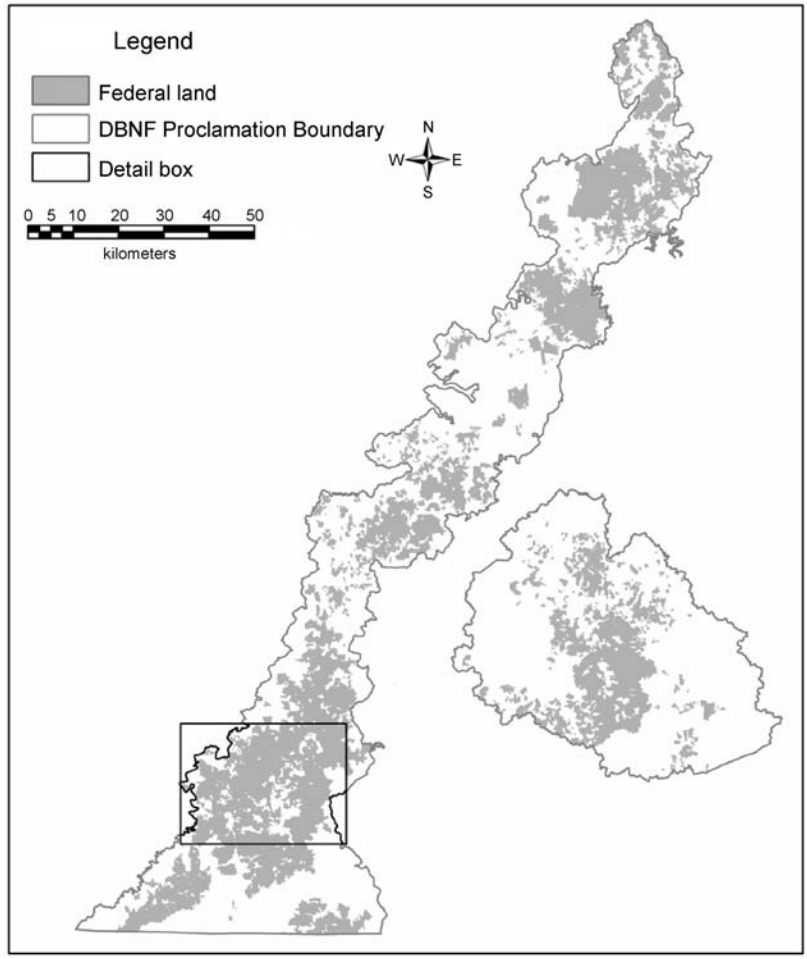

Fig. 1. Distribution of federal lands within the Daniel Boone National Forest (DBNF). The detail box represents the area that will be shown in more detail in later figures.

differencing, image ratioing, and vegetation index differencing in detecting gypsy moth defoliation using multidate Landsat MSS data. A difference of the near-infrared/red ratio was found to be more useful in delineation of defoliated areas than any single band-pair difference or ratio. This technique had an accuracy of about 78%. In another study conducted in Pennsylvania using Landsat MSS data, Williams and Nelson (1986) found a ratio of MSS7 (NIR) and MSS5 (red) to be useful in accurately delineating heavily damaged forest stands (i.e., 60–100% canopy removed) from relatively healthy stands. However, they found moderate defoliation and healthy forest to be spectrally inseparable.

Vogelman and Rock (1989) used two-date Landsat TM images to map hardwood forest damage by pear thrips in Vermont and Massachusetts. Their results indicated that ratio indices of Landsat TM5 (MIR) and TM4 (NIR) when used in combination with image differences of the same bands were able to distinguish between low- and

high-level damage areas. In another study, Muchoney and Haack (1994) evaluated the suitability of merged principal components analysis, image differencing, spectral-temporal change classification, and post-classification differencing for detecting forest defoliation. They concluded that defoliation was best determined using image differencing and principal components analysis, which had accuracies of 74% and 68%, respectively. Lambert et al. (1995) used logit regression and Landsat TM data to differentiate between three damage classes of Norway spruce. They found TM3 best at delineating heavy damage, whereas TM1, TM4, and TM7 when used together were able to distinguish between light and moderate damage. Ekstrand (1996) integrated Landsat TM data with elevation and forest stand data to separate slight defoliation from moderate defoliation of Norway spruce, and obtained an accuracy of 85% in flat terrain and 75% in hilly terrain.

In another study utilizing multidate Landsat TM data, Collins and Woodcock (1996) compared Kauth-Thomas and principal components (PC) transforms with Gramm-Schmidt orthogonalization for mapping pest-induced forest mortality in the Lake Tahoe Basin. They concluded that the KT transformation was most sensitive to changes in vegetation condition. Royle and Lathrop (1997) examined defoliation changes in eastern hemlock using Landsat TM data, TM4/TM3 ratio, and regression analysis. They obtained an overall accuracy of 64% with four defoliation classes, 70% with three classes, and 78% with two classes. Ardo et al. (1997) used neural networks with multitemporal Landsat TM data for classifying Norway spruce damage and obtained an accuracy of 78%.

Falkenstrom and Ekstrand (2002) used the IRS-1c Linear Imaging Self-Scanning Sensor 3 (LISS-3) to assess slight and moderate defoliation in Norway spruce– and Scots pine–dominated boreal forests. IRS-1c–derived damage maps were found to be of equivalent accuracies to those obtained using Landsat TM data. They also found the NIR band to be best correlated with spruce defoliation especially after applying topographic normalization to the data. Pine damage was best correlated with the NIR/Red ratio and NDVI.

Skakun et al. (2003) used multitemporal Landsat ETM+ data to map lodgepole pine forest damage by mountain pine beetle in British Columbia, Canada. They used three-date Tasseled Cap wetness images to generate an enhanced wetness difference index. This index was then used to map two classes of red-attack damage in lodgepole pine, with accuracies ranging from 67% to 78%.

Topographic Normalization

In regions of rugged topography such as the DBNF, information about the land surface on a satellite image may be obscured by changes in illumination and reflection geometry. These changes caused by different slope angles and orientations make similar surfaces appear different (brighter or darker). Topographic normalization techniques strive to reduce differences in illumination for the same land-cover types, thereby allowing classification of land-cover types with less confusion and more accuracy.

Image ratioing has been used as an alternative method for reducing topographic effects, but this method does not take into account the physical behavior of scene elements. Early topographic correction models were based on the Lambertian model,

which assumes that incident solar radiation is reflected equally in all directions. Using this technique, satellite images were normalized according to the cosine of the effective illumination angle (Smith et al., 1980). However, most natural surfaces behave as non-Lambertian reflectors, and the cosine correction had to be extended by introducing parameters that simulate the non-Lambertian behavior of the surface (Civco, 1989; Colby, 1991). The estimation of these parameters is based on a linear regression between the radiometrically distorted bands and a shaded terrain model. Among the non-Lambertian topographic normalization techniques are the Statistic-empirical method, Minnaert correction, and C-correction (Teillet et al., 1982; Meyer et al., 1993). McDonald et al. (2002) evaluated the performance of the Statistic-empirical method, Minnaert correction, and C-correction and concluded that: (1) the C-correction provided the best reduction in illumination-driven variation observed in areas of similar cover type; and (2) increased separation of spectrally similar classes of forests.

Decision Tree Classification

Traditional land-cover mapping techniques have used differences in spectral reflectance properties of earth materials to distinguish between vegetation, water, soil, and urban features. In recent years, more advanced techniques have improved the level of detail that can be extracted from satellite-based image data. Hutchinson (1982) outlined the incorporation of ancillary data sources (e.g., elevation data) into the mapping process and Strahler et al. (1978) included elevation data, such as slope and aspect to improve forest map accuracy. More recently, techniques such as spectral mixture modeling (Roberts et al., 1998; Rogan et al., 2002) and decision trees have been used to improve mapping accuracies (Friedl and Brodley, 1997, de Colstoun et al., 2003).

Decision tree classification has been implemented in numerous software packages and is widely used in remote sensing applications (DeFries et al., 1998; Friedl and Brodley, 1997; Friedl et al., 1999; Hansen et al., 2000; Huang and Townshend, 2003; Lawrence and Wright, 2001; Hodgson et al., 2003). Decision tree classifiers are non-parametric and therefore independent of the distribution of the class signature, can handle both continuous and categorical data, generate interpretable classification rules, and are fast to train and often as accurate as or more accurate than other classifiers (Hansen et al., 1996; Friedl and Brodley, 1997; Huang et al., 2002a).

Modeling within the decision tree analysis is accomplished through a recursive binary partitioning of training data sampled from various imagery sources, so that values are representative of the entire data set (Quinlan, 1993). These samples are then used in the production of rule sets, based on the relationships modeled, essentially enabling the software to build a knowledge base with little interaction or input required from the user. Based upon the training samples, the decision tree software is able to approximate the human learning process and make accurate generalizations concerning the relationships of input variables and the value of the target feature (Herold et al., 2003).

Image Enhancements/Transformations

The normalized difference index (NDVI) has been the most widely used index in global vegetation studies (Goward et al., 1985; Townshend et al., 1994). NDVI has

been extensively used to obtain information about biophysical parameters such as leaf-area index (Jordan, 1969), biomass (Anderson et al., 1993), and photosynthetic activity (Myneni et al., 1997). NDVI has been shown to be sensitive to changes in soil reflectances, to be perturbed by atmospheric effects, and to saturate in forested sites (Huete et al., 1994). As a result, alternative vegetation indices that are less sensitive to these perturbations have been developed. These include the soil and atmosphere resistant vegetation index (SARVI2) based on the modified normalized difference vegetation index (MNDVI). The MNDVI incorporates soil adjustment and atmospheric resistance concepts into a feedback-based equation (Liu and Huete, 1995). SARVI2 is a simplified form of MNDVI in which the requirement that it be expressed in terms of NDVI has been eliminated (Huete et al., 1997). SARVI2 is calculated as follows:

$$SARVI2 = 2.5\frac{\rho NIR - \rho RED}{1 + \rho NIR + 6\rho RED - 7.5\rho BLUE},$$

where p is top-of-the-atmosphere reflectances. NDVI has been shown to be sensitive to and respond primarily to the highly absorbing red reflectance band, while SARVI2 is more responsive to variations in the near-infrared (NIR) and, unlike NDVI, does not saturate over forested sites (Huete et al., 1997).

The transformation of the raw satellite images using principal components analysis (PCA) can result in new principal component images that may be more interpretable than the original data (Singh and Harrison, 1985). In addition PCA is used to reduce data dimensionality through compression of multispectral data to a few component images. The principal components can be standardized by a correlation matrix instead of a covariance matrix (Singh and Harrison, 1985; Fung and LeDrew, 1987). PCA can be used for land-cover change detection (Bryne et al., 1980; Singh, 1989; Singh and Harrison, 1985). This technique involves using two dates of data to create new images that are uncorrelated with each other. The new principal components are orthogonal to each other such that the first component contains most of the variance in the original data, with each succeeding band containing increasingly less variance than the original data. It can be difficult to associate physical scene characteristics with individual components produced using multidate principal components, as they are scene dependent (Seto et al., 2002). Both Fung and LeDrew (1987) and Eastman and Fulk (1993) indicated that standardized PCA was more effective than unstandardized PCA for change detection.

The Tasseled Cap transformation (KT transformation) was originally constructed for understanding important phenomena of crop development in spectral space (Kauth and Thomas, 1976). The transformation is useful for compressing spectral data into a few bands associated with physical scene characteristics (Crist et al., 1986). The KT transformation has found widespread applicability throughout the field of remote sensing. KT transformation has potential applications in revealing key forest attributes including species, age, and structure (e.g. Cohen et al., 1995) and has been shown to facilitate accurate mapping of forest cover and forest disturbances (Cohen et al., 1998).

Change Detection

Numerous digital change detection techniques have been developed. These include image differencing (Muchoney and Haack, 1994), image regression (Jha and Unni, 1994), image ratioing (Prakash and Gupta, 1998), vegetation index differencing (Nelson, 1983, Townshend and Justice, 1995), principal components analysis (Bryne et al., 1980, Jha and Unni, 1994; Kwarteng and Chavez, 1998), spectral-temporal classification (Weismiller et al., 1977; Muchoney and Haack, 1994; Bruzzone and Serpico, 1997), post-classification comparison (Jensen et al., 1987; Mas, 1999; Foody, 2001), and change vector analysis (Sohl, 1999).

Univariate image differencing is the most widely applied change-detection algorithm and involves the subtraction of one date of an original or transformed image from a second date that has been previously registered to the first. The difference image should contain positive and negative values that represent change and zero values that represent no change (Coppin et al., 2004). Threshold values to indicate whether significant or relevant change has occurred need to be defined and are often set interactively using multiples of a residual standard deviation.

Image ratioing involves a pixel-by-pixel division of pixels from one date with those from another date. A pixel that has not changed will yield a ratio value of one, and those that have changed will have either higher or lower values than one (Coppin et al., 2004). The resulting ratioed image often has a non-Gaussian bimodal distribution and therefore the standard deviation cannot be used for threshold definition (Riordan, 1981).

Post-classification comparison involves pixel-by-pixel comparison of independently produced classification results from each two time periods, and results in a complete matrix of change. Other advantages of this technique are that radiometric differences between dates are minimized through the independent classifications. The main disadvantage of post-classification comparison is that its accuracy may be low because it is totally dependent on the accuracy of individual classifications. Misclassifications and mis-registration errors present in the original images are compounded using post-classification comparison (Howarth and Wickware, 1981).

Spectral-temporal change classification is based on single analysis of a merged multidate data set using standard pattern recognition and classification techniques. This technique requires numerous spectral classes be generated and labeled, but this may be difficult unless the analyst is intimately familiar with the study area (Jensen, 1983).

In bi-temporal linear data transformation, data sets from two dates are stacked together in a single image and a linear data transformation such as PCA or Tasseled Cap applied. The premise for this analysis using PCA is that multitemporal data sets are highly correlated and that PCA can be used to highlight differences attributable to change (Bryne et al., 1980; Muchoney and Haack, 1994). Coppin et al. (2004) indicated that localized changes were enhanced in lower components of a multitemporal PCA when the major portion of the variance in the multitemporal sequence was unchanged (constant) land cover. Fung and LeDrew (1987) found standardized PCA superior to unstandardized PCA because its PCs were aligned better along change. Singh and Harrison (1985) found standardized PCA resulted in substantial improvement in signal-to-noise ratio compared to unstandardized multidate PCA.

KT transformation has been found effective in change detection studies for mapping forest mortality (Collins and Woodcock, 1996). KT transformation applied to a 12-band Landsat TM data will yield change in brightness, greenness, and wetness bands in components 7, 8, and 9, respectively. Unlike PCA, multidate KT transformation is scene independent and has been shown to be successful in identifying change in an understandable and consistent manner (Fung, 1990; Collins and Woodcock, 1996).

DATA AND METHODS

Study Area

The Daniel Boone National Forest (DBNF) is located in the mountains of eastern Kentucky and consists of approximately 284,000 ha of federally administrated land within an 850,000 ha Proclamation Boundary (Fig. 1). This land is generally rugged and characterized by steep forested ridges, narrow valleys, and over 5,400 km of cliffline.

The Daniel Boone National Forest falls within the mixed mesophytic region of the Eastern Deciduous Forests and is characterized by a wide variety of species both in the understory and in the overstory (Braun, 1950). Among the species found in the canopy layer on the north and east slopes and in coves are northern red oak, basswood, beech, yellow poplar, sugar maple, birch, red maple, and hemlock. West slopes contain yellow poplar, red oak, white oak, and hickories. On the south slopes and on the ridges, where moisture becomes more limiting, is an association of short leaf pine, chestnut oak, white oak, and Virginia pine. Stands of yellow pine are composed primarily of shortleaf pine, with pitch pine, and Virginia pine. There are also some planted areas of loblolly pine. Pine forest types occupy 15% of the forest area. Another 12% of the forest area is classified as either pine-hardwood or hardwood-pine, depending on which component constitutes a majority. White pine occurs in combination with other species, and comprises less than l% of the total forest area (DBNF, 1999).

Data: Image Acquisition Issues

A complete coverage of the DBNF proclamation boundary area requires three Landsat scenes acquired along the World Reference System (WRS-2) path 19 and rows 33, 34, and 35 (Fig. 2). We chose leaf-off pre- and peak-outbreak images for this study because our primary interest was with conifer species that are prominent during this time while hardwood species are dormant. Mapping forest damage by SPB required the development of an accurate conifer species map, which would be difficult to produce using leaf-on (e.g., summer images) because of a higher probability of confusion between hardwood and conifer species.

It was also important that the images to be used in the change detection be anniversary or near-anniversary (Jensen, 1996). Anniversary images are acquired at approximately the same period in the year when illumination, weather, and phenologic conditions in the scene are likely to be most comparable. Leaf-off images acquired at higher sun elevations were preferred over leaf-off images acquired under

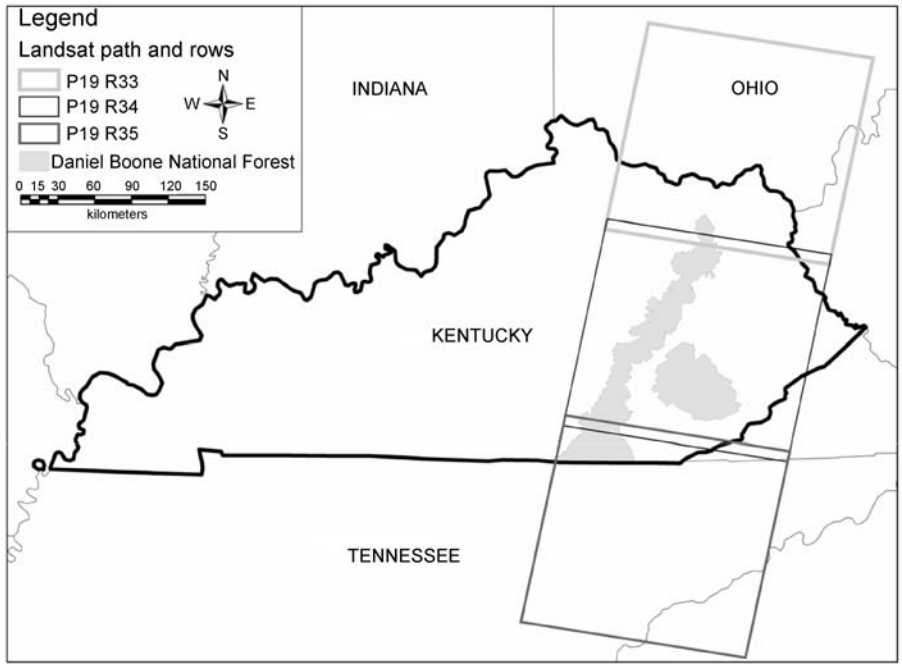

Fig. 2. Location of the Daniel Boone National Forest in eastern Kentucky and the Landsat WRS-2 scenes necessary for a complete coverage.

lower sun elevations because of the reduced shadowing associated with higher sun angles. Images acquired in November through February have lower sun angles compared to images acquired in March and April. Care had to be exercised in not delaying image acquisition beyond the first 10 days of April because in eastern Kentucky, deciduous vegetation starts to green-up significantly.

The first reports of SPB outbreak within the DBNF were made by field foresters in the summer of 1999. The desired pre-SPB breakout images would have been those acquired in March or April of 1999 (leaf-off period for hardwoods) because conifers are most prominent and topographic shadowing is less pronounced. Unfortunately, the closest three-scene data set of cloud-free images for the study area were acquired on board Landsat 5 on March 15, 1995 and there was little choice but to use these as pre-outbreak images. There was little concern that these images had been acquired four years earlier than the desired date because there had been little forest disturbance within the DBNF in the intervening period (a logging ban has been in place since early 1990s). The peak-SPB breakout images were acquired on board Landsat 7 on March 10, 2002.

Other data used in this research included color infrared photography acquired in July 2001 at a scale of 1:20,000, and a 10 m Digital Elevation Model (DEM). In addition, point and polygon coverages of SPB-damaged forest stands and those for stands that appeared healthy and unaffected by SPB outbreak were used. The point data had been created from SPB-damaged forest stand locations acquired using differential GPS during the summer of 2001 and spring of 2002. Polygon coverages of

SPB-damaged forest stands and healthy stands were obtained through aerial sketch mapping by United States Forest Service crews in 2001. Other data used in this research included forest stand data for the federally administered portion of the DBNF, and vector data including the DBNF Proclamation boundary, streams, and state and local roads.

Image Processing

Geometric, Radiometric, and Topographic Corrections. The three Landsat ETM+ images acquired on March 10, 2002 were precision-corrected and did not require georeferencing. The pre-SPB outbreak images acquired on March 15, 1995, however, were not georeferenced; therefore each of the three Landsat TM images was georeferenced to its corresponding Landsat ETM+ image. Georeferencing was implemented using at least 20 ground control points (GCPs), a first-order polynomial, and nearest neighbor resampling, and resulted in a total root mean square (RMS) error of less than half a pixel (15 m).

After georeferencing, the three Landsat TM and three Landsat ETM+ images were mosaicked. As over 85% of the DBNF Proclamation area lies within the image acquired along path 19 row 34, this image was made the reference in the mosaic process. The histograms of image subsets acquired along path 19, row 33 and path 19, row 35 were made to match those of the image acquired along path 19, row 34, and then created image mosaics for 1995 and 2002 (Fig. 3).

Landsat 5 TM and Landsat 7 ETM+ data are very similar and can be used interchangeably when cross-calibration is applied. Vogelmann et al. (2001) developed regression equations to convert ETM+ DN values to Landsat 5 TM DN values. In order to take advantage of the superior radiometric calibration of Landsat ETM+ compared to Landsat TM, Huang et al. (2002c) developed reverse regression equations for converting TM DN values to ETM+ DN equivalents. We therefore used these regression equations to convert DN values for the March 15, 1995 Landsat TM image mosaic to the equivalent ETM+ DN values. We then subjected the 1995 and the 2002 image mosaic to radiometric and atmospheric corrections using Landsat ETM+ gains and offset values, the dark object subtraction method (Moran et al., 1992), and the COST method (Chavez, 1996). These methods are entirely image based and have been found to be as accurate as methods that use *in situ* atmospheric field measurements and radiative transfer codes (Fig. 3).

It was necessary to apply topographical normalization to the resulting images because of the highly rugged topography of eastern Kentucky. Topographically normalized images (Fig. 4) were generated using the C-correction method (Teillet et al., 1982) and a 10 m DEM that had been resampled to 30 m. We then applied a mask derived from the DBNF Proclamation boundary to extract from each image mosaic (1995 and 2002) only those pixels that fell within this boundary.

Image Enhancements and Ancillary Data. We applied several image enhancements to the 1995 Landsat TM image for input, together with other ancillary data, in a decision tree classification of conifer species within the DBNF. The Landsat TM image was transformed into PCA images, KT brightness, greenness, and wetness images using at-satellite Tasseled Cap coefficients derived by Huang et al. (2002b) and SARVI2 images. The DEM was used to create a slope and aspect image, whereas the

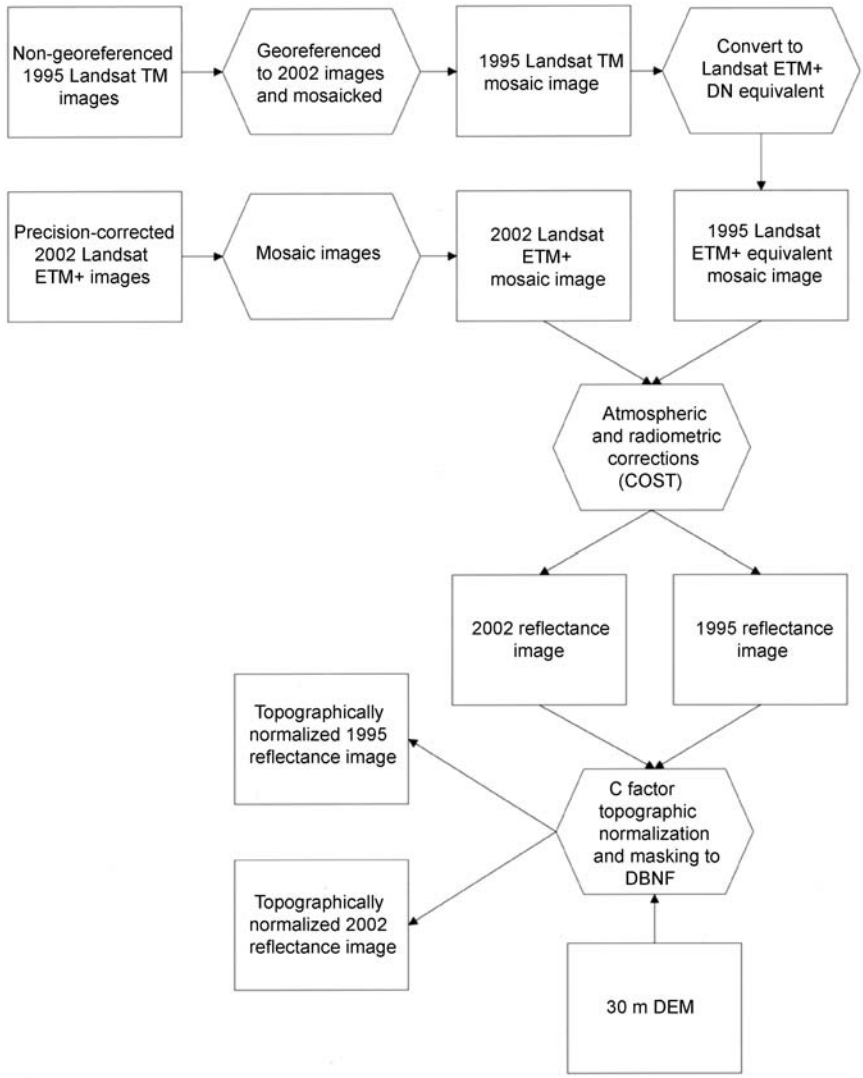

Fig. 3. Geometric, atmospheric, and radiometric processing of the 1995 and 2002 Landsat TM and ETM+ images.

streams and river coverage were used to compute a "distance from rivers and streams" image (Fig. 5). This distance image was thought to be useful in delineating hemlock species from pine species, since hemlock stands tend to be located along drainages.

Ten color infrared (CIR) photos acquired in July 2001 at a scale of 1:20,000 were scanned at an optical resolution of 800 dpi. Each photo was then orthorectified into the State Plane Coordinate System using 12–20 control points, a 10 m DEM, and camera calibration coefficients. Control points were obtained from Digital orthophoto quarter quads (DOQQ) with a spatial resolution of 1 m. Each digital photo was orthorectified to within a total RMS error of less than one pixel.

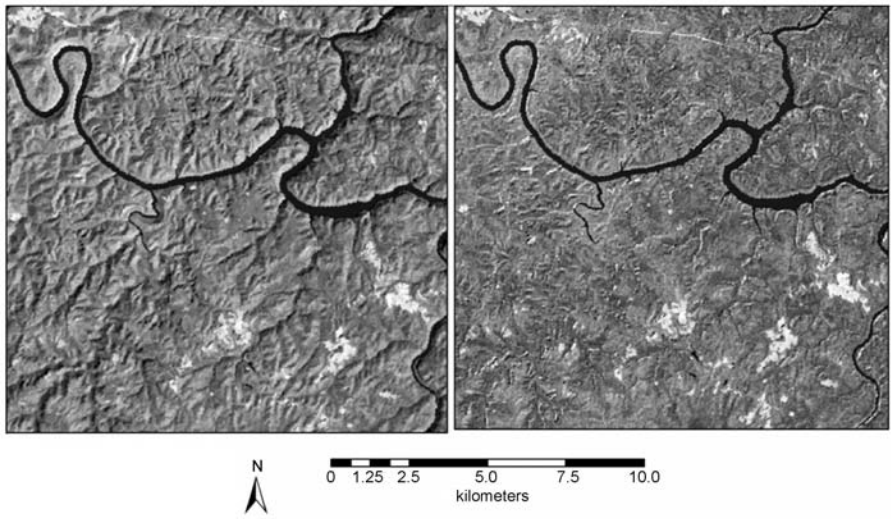

Fig. 4. Landsat TM image acquired in 1995 for a portion of the DBNF before (left) and after (right) topographic normalization.

Decision Tree Conifer Species Mapping

We first created an evergreen species map using an image composite consisting of 1995 Landsat TM bands and a SARVI2 image and ISODATA unsupervised classifications (Tou and Gonzalez, 1974; Sabins, 1987). Because this image was acquired in the winter, only the evergreen forest species, winter agriculture, and pasture appeared green in the image and therefore needed to be separated. We found adding a SARVI2 to the six TM reflective bands and running unsupervised classifications greatly improved the separation of evergreen forest pixels from pasture and agriculture pixels (Fig. 5). The evergreen forest map created was then used to extract evergreen forest pixels from all input data that were to be used in the construction of decision tree classifier.

We used the See5 (C5) decision tree classification program (RuleQuest Research, 2001) to create a conifer species map consisting of white pine, shortleaf pine, Virginia pine, and hemlock. The See5 program searches for an accurate decision tree to predict an array of training cases. The decision tree is simplified and converted to production rules where each rule is composed of if-then statements (Hodgson et al., 2003). Each rule is composed of one or more conditions, all of which must be met for the rule to be evaluated as true. The program employs an information gain ratio method in tree development and pruning, and has many other features including boosting and cross-validation (RuleQuest Research, 2001).

Construction of a decision tree classifier for mapping conifer species required that we use training samples representative of the four conifer species targeted for mapping (shortleaf pine, Virginia pine, white pine, and hemlock). Training samples were obtained from two sources: existing forest stand data (also known as Continuous Inventory and Stand Condition [CISC] data), and field-derived forest stand data gathered in 2002. Existing forest stand data are only available for federally administered

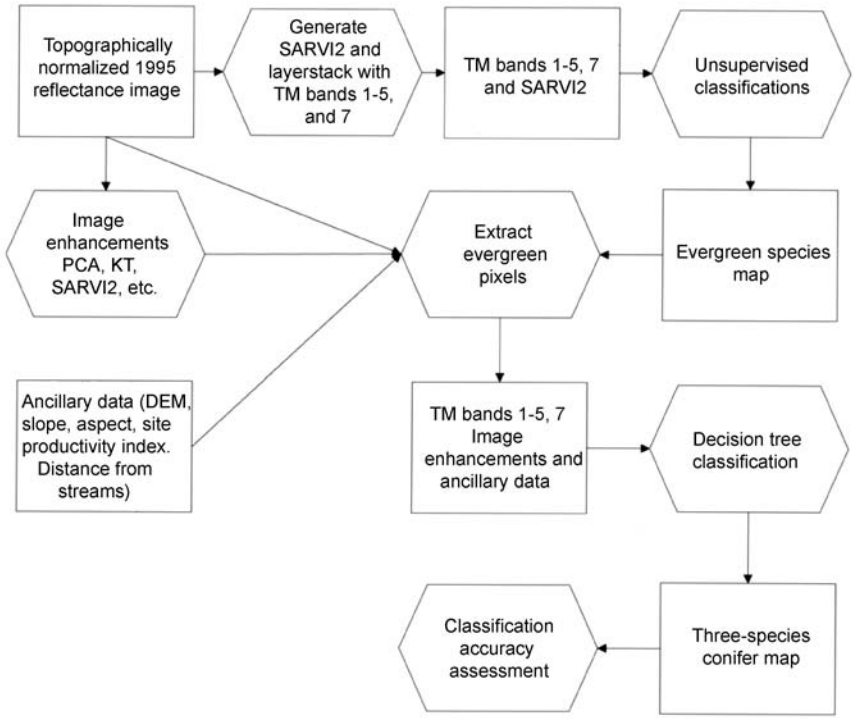

Fig. 5. Creating a conifer species map for 1995 using a decision tree classifier.

lands within the DBNF, whereas the field-derived data were available for both federal and private lands. Field data obtained in 2002 were gathered using sample plots ranging in size between 0.4 and 1.6 ha. Before these samples could be used to train the decision tree classifiers, we overlaid these plots on existing forest stand data in order to ensure that the forest stands in these sample plots had been in existence in 1995. We also examined stand history data from CISC data to ensure that sample plots selected for this analysis had not undergone modification (e.g., logging) between 1995 and 2002. This was necessary because the sample plots would be used to train a decision tree classifier for the 1995 pre-SPB outbreak image. For a forest stand to be designated as one of the pine species or hemlock, it had to have at least 70% of its dominant and co-dominant basal areas belonging to that pine species or hemlock.

Many independent variables were input into See5 to create a decision tree classifier. See5 has a "winnowing" option that keeps only those variables determined to provide meaningful information in the construction of a decision tree or ruleset. Variables retained for constructing decision trees were: DEM, slope, KT greenness, KT wetness, TM1, TM4, Site productivity index, Distance from streams, PCA3, and PCA4. Training data were internally evaluated using 50% testing blocks that were kept separate from the tree-building process. Internal evaluation of the classifier indicated there was great confusion between Virginia pine and shortleaf pine. For this reason, training data for the two species were merged to form a Shortleaf/Virginia pine

Table 1. Error Matrix of the 1995 Conifer Species Map

Classified data	Reference data			Classified total
	1	2	3	
1. White pine	3,136	223	527	3,886
2. Hemlock	237	1,658	532	2,427
3. Shortleaf pine/Virginia pine	770	943	10,078	11,791
Reference total	4,143	2,824	11,137	18,104

Land cover class	Reference totals	Classified totals	Number correct	Producer's accuracy	User's accuracy
1. White pine	4,143	3,886	3,136	75.7	80.7
2. Hemlock	2,824	2,427	1,658	58.7	68.3
3. Shortleaf pine/Virginia pine	11,137	11,791	10,078	90.5	85.5
Total[a]	18,104	18,104	14,872		

[a]Overall classification accuracy = 82.1%; kappa statistic = 0.663.

class and See5 run again. Evaluation of the resulting decision tree classifier for the three conifer species had an error of less than 20% using test data excluded from building the decision tree. This classifier was then applied to the 1995 image to produce a detailed conifer map (Fig. 5).

RESULTS AND ANALYSES

Conifer Species Map Accuracy Assessment

An accuracy assessment was performed on the resulting three-species conifer map using forest stand data and field data that had not been used in creating the decision tree classifier. The overall accuracy of the conifer map was 82.1% (Table 1). The Shortleaf/Virginia pine class had the highest classification accuracy, with both producer's and user's accuracy over 85%. Hemlock had the lowest classification accuracy with only 58.7% of the hemlock species class (in the reference) correctly identified as hemlock on the map, while only 68.3% of all areas labeled hemlock on the map were actually hemlock on the ground. The dominant conifer species is the shortleaf pine/Virginia pine class comprising of over 75% of all conifer species within the DBNF Proclamation boundary (Table 2).

Much of the mapping confusion was between hemlock and shortleaf pine. One reason for the lower classification accuracy of the hemlock can be attributed to CISC data that may not have been current, or had been derived using insufficient field data. It may be possible to separate shortleaf pine from Virginia pine reliably in the future by using more field sample plots and higher quality field data. The decision tree classifier performed remarkably well and for the first time there is now a preliminary map of three conifer species associations in the DBNF.

Table 2. Conifer Forest Species Area Summaries for Federal and Private Lands within the Daniel Boone National Forest, 1995

Species	Federal lands, ha	Percent of federal	Private lands, ha	Percentage private
White pine	6,478.3	8.5	656.7	1.0
Hemlock	12,560.7	16.4	13,118.2	18.7
Shortleaf/Virginia pines	57,417.7	75.1	52,552.0	80.3
Total	76,456.7	100.0	66,326.9	100.0

Land Cover Change Mapping

The second part of the study involved evaluating the suitability of five change-detection techniques for mapping SPB-induced forest damage in the DBNF. The first two change-detection techniques evaluated involved a bilinear data transformation of stacked 1995 and 2002 Landsat TM and ETM+ reflectance bands using both standardized and unstandardized PCA, and followed by unsupervised classifications (see Fig. 7). The other techniques evaluated involved spectral-temporal change classification of merged multidate data sets followed by unsupervised classification techniques. These merged data sets consisted of the various KT-transformed images (brightness, greenness, and wetness) and SARVI2 images for 1995 and 2002.

No attempt was made to delineate SPB-induced forest damage classes because conifer mortality was very high (over 90%) in most stands we visited. We found that many of the conifer stands that we had assigned "light" or "moderate" damage in spring and summer of 2001 had degenerated to "heavy" mortality during our next field visit in spring 2002. It is therefore important that designation of forest damage classes in the field data be conducted as closely as possible to acquisition of post-damage or peak-damage image.

Multitemporal PCA Change Mapping. Steps necessary to implement this change detection are summarized in Figure 6. We began by creating a 12-band composite image consisting of bands 1–5 and 7 from both the 1995 Landsat TM and the 2002 ETM+ image. Both standardized PCA (using correlation matrices) and unstandardized PCA (using variance-covariance matrices) were applied to the 12-band image composite. A 12-band output PCA image was created for each PCA technique. Each PC output was then examined for information on land cover change and no change between 1995 and 2002. In order to be able to identify PCA image associated with change and no change, we overlaid each image with polygons representing conifer stands damaged by SPB, and those that had remained unchanged between 1995 and 2002 (i.e., healthy stands). SPB damaged conifer stands and healthy stands had been identified and created earlier using field data and orthorectified CIR photos obtained in 2001.

For both standardized and unstandardized PCA output images, we identified PC 4 to be associated with unchanged conifer stands, whereas PC 6 and PC 7 were associated with conifer damage by SPB. Unchanged conifer stands in PC 4 appeared bright in both SPCA and UPCA images. PC 4 had heavy positive loadings in TM4 and ETM+4 (NIR band) and heavy negative loadings in both TM3 and ETM+3 (red

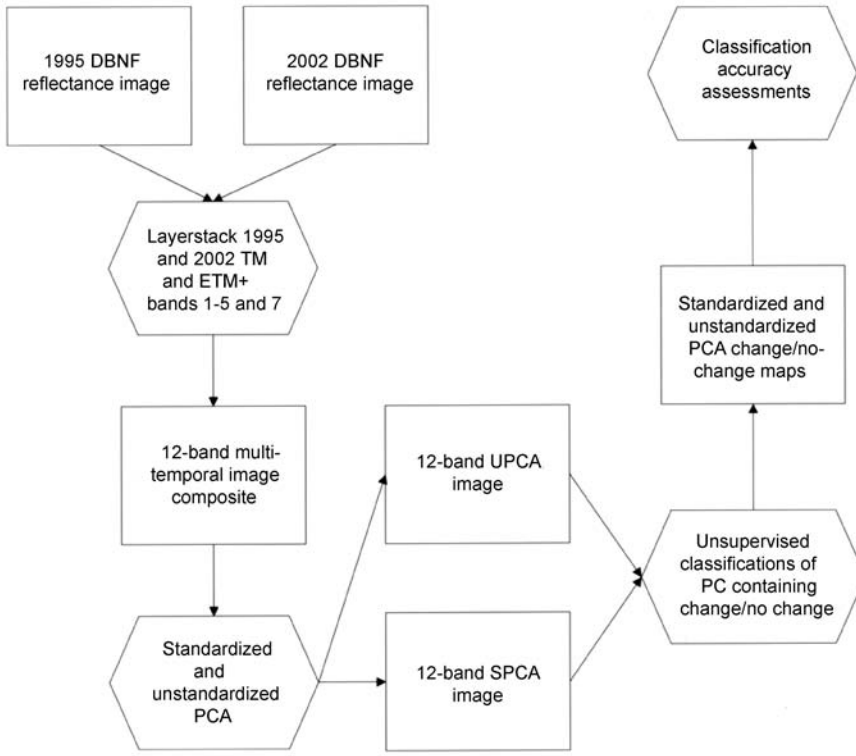

Fig. 6. Image processing steps used to implement standardized and unstandardized PCA change detection using merged multitemporal Landsat TM and ETM+ data.

band). Healthy vegetation has a high reflectance in the NIR band and a low reflection in the red band. As a result, forest stands that remained healthy between 1995 and 2002 appeared bright in PC4. SPB damaged stands appeared dark in PC6, which had heavy positive loadings in TM1 and ETM+1 and a negative loading in TM3. Damaged conifer stands have a higher red reflectance compared to healthy stands because of reduced photosynthetic activity, and therefore appeared dark in PC6. SPB-damaged conifer stands appeared bright in PC7, which had heavy positive loadings in TM4 and heavy negative loadings in ETM+4. PC7 therefore contrasts NIR reflectance between 1995 and 2002. Damaged conifer stands had a lower NIR reflectance in 2002 compared to 1995, and therefore appeared brighter in PC 7. When PCA bands 4, 6, 7 were displayed as RGB, pixels associated with conifer damage appeared in pink tones whereas unchanged pixels appeared in blue tones (Figs. 7A and 7B). PC4, 6, 7 accounted for only 0.89%, and 0.85% of the total variance observed in the standardized and unstandardized PCs, respectively. ISODATA unsupervised classifications were used to develop a conifer damage/no damage map from the three-band image composite consisting of PC4, PC6, and PC7.

SARVI2 Change Detection. The SARVI2 change detection mapping involved creating a two-band image composite consisting of SARVI2 images for 1995 and 2002. The red color gun was used to display the 1995 SARVI2, whereas the green

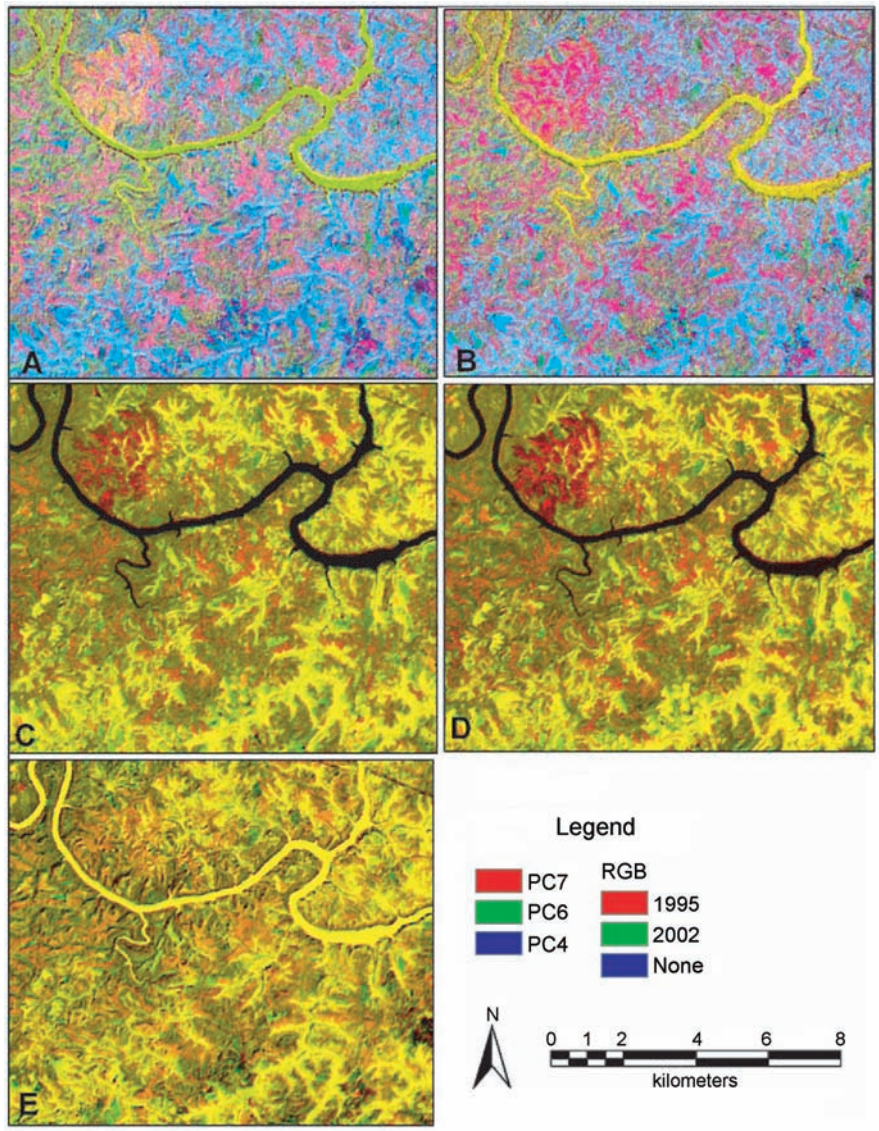

Fig. 7. Image composites illustrating the five change-detection techniques evaluated. A. SPCA. B. UPCA. C. SARVI2. D. KTG. E. KTW.

color gun displayed the 2002 SARVI2 image. The blue color gun was turned off. Pixels that experienced a decrease in SARVI2 brightness (and consequently conifer damage by SPB) between 1995 and 2002 appeared in red tones whereas unchanged pixels appeared in yellow tones (Fig. 7C). A conifer damage/no-change map was subsequently created from the two-band SARVI2 composite using ISODATA unsupervised classifications.

Multidate KT Change Detection. The third change detection technique evaluated involved the Tasseled Cap (KT) transformation. KT brightness, greenness, and

wetness (KTBGW) images for 1995 had been created earlier for input in developing the conifer species map. KT transformation using at-satellite reflectance tasseled coefficients derived by Huang et al. (2002b) was applied to the 2002 Landsat ETM+ image to create KT brightness, greenness, and wetness images. Next, we stacked in pairs KT brightness, greenness, and wetness images for 1995 and 2002 images. The KT brightness (KTB) pair consisted of the KT brightness image for 1995 and the KT brightness image for 2002. Likewise, the KT greenness (KTG) pair consisted of the 1995 and 2002 greenness images, and the KT wetness (KTW) image pair consisted of the wetness images from 1995 and 2002.

The red color gun was used to display the 1995 KTB image and the green color gun to display the 2002 KTB image, while turning off the blue color gun. Using this display, pixels that experienced a decrease in brightness between 1995 and 2002 appeared in red tones while those that experienced an increase appeared in green tones. Pixels that remained unchanged in brightness appeared in yellow tones. KT brightness images displayed in this manner did not appear to be related to SPB-damaged conifer stands and so KTB was not given further consideration.

KTG and KTW images were displayed as described for KTB. Pixels that experienced a decrease in greenness or wetness between 1995 and 2002 appeared in red tones, while those in which greenness or wetness increased appeared in green tones. Yellow tones represented pixels in which greenness or wetness remained unchanged between 1995 and 2002 (Figs. 7D and 7E). Decreases in KTG and KTW images (red color tones) appeared to be related to a reduction in the amount of green vegetation and canopy between the two image dates. Unsupervised classification techniques were used to create conifer damage/no-change maps from the KT greenness and KT wetness band pairs.

Accuracy Assessment of Forest Damage Maps

Five land-cover change maps were produced: from multitemporal standardized PCA and unstandardized PCA, from multidate KTG and KTW, and from multidate SARVI2. Since the mapped changes included non-conifer areas, we applied the evergreen species mask created earlier to retain only those change pixels that fell within evergreen forest area. In order to decide which of the five change-detection methods used to produce conifer damage/no-change maps was best, an accuracy assessment was performed. GPS-derived polygons representing SPB-damaged conifer stands and polygons for stands unaffected by the SPB were used. These polygons were produced using differential GPS during 2001–2002.

Additional polygons representing conifer-damaged stands were digitized from orthorectified CIR photos obtained in August 2001. SPB-damaged forest stands in orthorectified CIR images appeared in greenish blue tones, and these were digitized into approximately 600 polygons. These polygons were combined with field-derived polygons and converted to a two-class raster image representing conifer stands damaged by SPB and those stands that did not change. This image was used as a reference in evaluating the accuracy of each of the five land-cover change maps by performing a pixel-by-pixel comparison. Classification error matrices, including the producer's, the user's, overall accuracy, and kappa statistics were computed for each conifer damage/no-change map created using each of the five change detection techniques (Table 3).

Table 3. Accuracy Assessments of Maps Derived Using Different Change-Detection Techniques in Mapping SPB-Induced Forest Damage[a]

	Reference data			User's accuracy, pct.
	1	2	Total	
SPCA classification[b]				
1	5505	26	99.5	
2	339	2389	87.6	
Total	5844	2415		
Producer's accuracy, pct.	94.2	98.9		
UPCA classification[c]				
1	4912	97	5009	98.1
2	333	2558	2891	88.5
Total	5245	2655	7900	
Producers' accuracy, pct.	93.7	96.3		
SARVI2 classification[d]				
1	4565	201	4766	95.8
2	120	1115	1235	90.3
Total	4685	1316	6001	
Producer's accuracy, pct.	97.4	84.7		
KT greenness classification[e]				
1	4484	679	5163	86.8
2	256	1719	1975	87.0
Total	4740	2398	7138	
Producer's accuracy, pct.	94.6	71.7		
KT wetness classification[f]				
1	4159	497	4656	89.3
2	143	1101	1244	88.5
Total	4302	1598	5900	
Producer's accuracy, pct.	96.7	68.9		

[a]Categories 1 and 2 represent conifer damage pixels and no-change pixels, respectively.
[b]Overall accuracy = 95.6%; kappa = 0.897.
[c]Overall accuracy = 94.6%; kappa = 0.881.
[d]Overall accuracy = 94.7%; kappa = 0.840.
[e]Overall accuracy = 86.9%; kappa = 0.693.
[f]Overall accuracy = 89.2%; kappa = 0.705.

Change Detection for Mapping Forest Damage

All five change-detection techniques resulted in overall classification accuracies above 86%. The standardized PCA (SPCA) change-mapping technique resulted in the highest classification accuracy followed closely by the unstandardized PCA (Table 3). These results are in agreement with those obtained by other researchers (Fung and

LeDrew, 1987; Eastman and Fulk, 1993; Eklund and Singh, 1993) who found standardized PCA to be superior to unstandardized PCA in change-detection studies. Standardized PCA uses the correlation matrix calculated from the *z*-scores of each image. Standardized PCA effectively forces all original input images to be of equal importance in the derivation of the output principal component images. The two principal component images highlighting conifer damage (PC6 and PC7) had high loadings in Landsat TM and ETM+ bands 4, 3, and 1. PC4 was had high loadings in the red and NIR bands (TM3, TM4, ETM+ 3, and ETM+4), and highlighted areas of no change.

Many studies utilizing satellite data to map forest damage have found a high correlation between forest damage and NIR reflection (e.g., Falkenstrom and Ekstrand, 2002). Change mapping using the SARVI2 vegetation index yielded the third-highest overall accuracy (Table 3). SARVI2 is calculated using bands 4, 3, and 1, and therefore the high accuracy attained using this vegetation index further confirms the importance of NIR, red, and blue regions of the electromagnetic spectrum in detecting forest damage. SARVI2 has been shown to be more responsive to variations in the near infrared (NIR) reflectance and, unlike NDVI, does not saturate over forested sites (Huete et al., 1997).

The KT greenness and KT wetness change mapping techniques had lower overall accuracies compared to the other three techniques, mainly because of higher omission errors in mapping the no-change classes (Table 3). KT greenness coefficients have highest weights in the NIR and red bands, thus making KT greenness similar to vegetation indices, although KT greenness has additional contributions from all other reflective Landsat bands. The KT wetness coefficients are highest in bands 5 and 7 (MIR), and therefore KT wetness is sensitive to changes in canopy conditions and stand structure (Cohen et al., 1995).

Based on the above results, either of the PCA techniques or the SARVI method would be appropriate for mapping SPB-induced conifer damage. The SARVI2 method is much easier to implement and interpret compared to the PCA techniques and is therefore recommended for use. Conifer-species damage maps derived from the standardized PCA change-detection technique indicated heavy pine mortality throughout federal and private lands of the DBNF, with approximately 84,500 ha damaged (Fig. 8). The heaviest conifer mortality was observed in the southern one-third of the DBNF, where the majority of pine stands are found. Mortality within the shortleaf/Virginia pine was highest at about 62%, while that in the white pines was approximately 52% (Table 4). It was surprising to see a large decrease in hemlock forest, as this is not a preferred host species for SPB. We believe that most of this damage actually occurred in the shortleaf/pine and white pine stands, which were incorrectly mapped as hemlock stands in the conifer map.

CONCLUSIONS

In this study, we constructed a decision tree classifier utilizing Landsat TM bands, image enhancements, and ancillary data to produce a three-species conifer species map. The pine species classes were classified with producer's and user's accuracies above 75%. Classification of the hemlock species remained problematic, with producer's and user's accuracies of 58.7% and 68.3%, respectively. The conifer-species

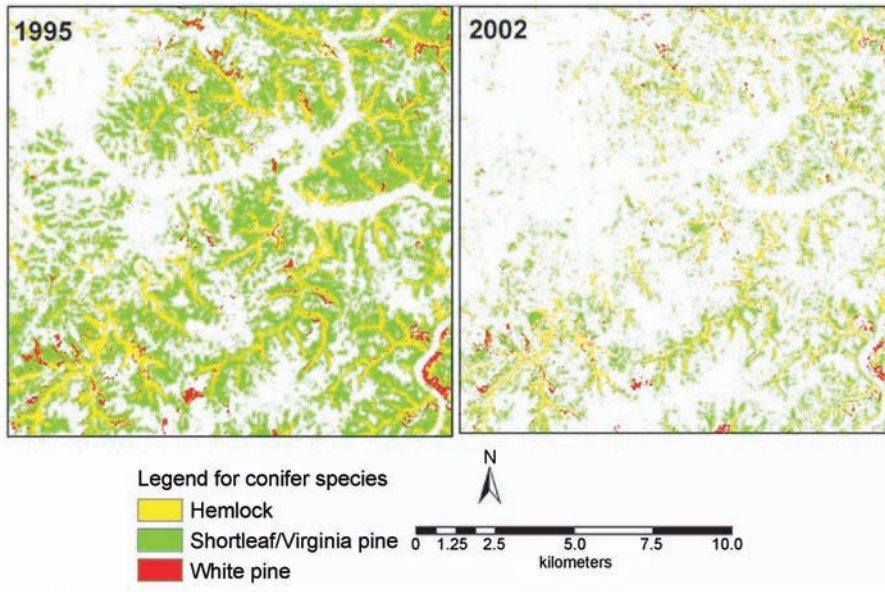

Fig. 8. Conifer species maps for a portion of the DBNF before (1995) and during (2002) peak SPB infestation.

Table 4. Change in Conifer Forest Area Attributed to SPB Mortality between 1995 and 2002

Conifer species	1995, ha	2002, ha	Percent change
White pine	7,135.0	3,393.9	52.4
Hemlock	25,678.9	11,007.5	57.1
Shortleaf/Virginia pines	109,969.7	42,233.4	61.6
Total	142,783.6	56,634.8	60.3

map could be improved by increasing the number and quality of field sample plots, and by incorporating topographic characteristics (landform indices) in decision tree classifications. Topographic characteristics can greatly influence microclimatic factors such as air and soil temperature, and moisture, and consequently growth, composition, and distribution of species (McNab, 1993). Results obtained in this study indicate that decision tree classifiers offer great promise in generating detailed forest species maps and in updating existing forest stand data. There is a need to identify more relevant ancillary data for input into decision tree classifiers that will be used to delineate more forest species at a higher accuracy.

The suitability of several change-detection methods for mapping insect-induced conifer damage was evaluated. All five change-detection techniques evaluated resulted in conifer-damage/no-change maps with overall accuracies greater than 86%. Standardized PCA emerged as the best-change detection procedure, followed very

closely by unstandardized PCA. The major disadvantage of using PCA in change detection is difficulty in interpreting the change components, as these are scene dependent. The SARVI2 change-detection technique is much easier to implement, more readily interpretable, and yields accuracies comparable to PCA change-detection techniques. We therefore recommend the SARVI2 change-detection approach for SPB forest-damage mapping in hardwood-conifer forest ecosystems.

ACKNOWLEDGMENTS

We are grateful to the staff at the Daniel Boone National Forest for their cooperation and field assistance. We thank Mr. James Brown, USDA Forest Health Protection Coordinator, Southern Region, for encouraging us to undertake this research project. We would also like to thank the anonymous reviewers who helped improve this paper. Funding for this research was provided by the USDA Forest Service, Forest Health Protection, under Grant no. 02-DG-11083150-110.

REFERENCES

Anderson, G. L., Hanson, J. D., and R. H. Haas, 1993, "Evaluating Landsat Thematic Mapper Derived Vegetation Indices for Estimating Above-Ground Biomass On Semiarid Rangeland," *Remote Sensing of Environment*, 45(2):165-175.

Ardo, J., Pilesjo, P., and A. Skidmore, 1997, "Neural Networks, Multitemporal TM Data and Topographic Data to Classify Forest Damage in the Czech Republic," *Canadian Journal of Remote Sensing*, 23(3):217-229.

Billings, R. F. and H. A. Pase, 1983, *A Field Guide for Checking Southern Pine Beetle Spots*, Washington, DC: USDA Agriculture Handbook No. 558.

Braun, E. L., 1950, *Deciduous Forests of Eastern North America*, Philadelphia, PA: Blakiston Company, 596 p.

Bruzzone, L. and S. B. Serpico, 1997, "An Iterative Technique for the Detection of Landcover Transitions in Multitemporal Remote Sensing Images," *IEEE Transactions on Geoscience and Remote Sensing*, 35(4):858-867.

Bryne, G. F., Crapper, P. F., and K. K.Mayo, 1980, "Monitoring Land Cover Change by Principal Component Analysis of Multitemporal Landsat Data," *Remote Sensing of Environment*, 10(3):175-184.

Chavez, J. P. S., 1996, "Image-Based Atmospheric Corrections—revisited and Improved," *Photogrammetric Engineering & Remote Sensing*, 62(9):1025-1036.

Civco, D., 1989, "Topographic Normalization of Landsat Thematic Mapper Imagery," *Photogrammetric Engineering & Remote Sensing*, 55(9):1303-1309.

Cohen, W. B., Fiorella, M., Gray, J., Helmer, E., and K. Anderson, 1998, "An Efficient and Accurate Method for Mapping Forest Clearcuts in the Pacific Northwest Using Landsat Imagery," *Photogrammetric Engineering & Remote Sensing*, 64(4):293-300.

Cohen, W. B., Spies, T. A., and M. Fiorella, 1995, "Estimating the Age and Structure of Forests in a Multi-Ownership Landscape of Western Oregon, USA," *International Journal of Remote Sensing*, 16(4):721-746.

Colby, J. D., 1991, "Topographic Normalization in Rugged Terrain," *Photogrammetric Engineering & Remote Sensing*, 57(5): 531-537.

Collins, J. B. and Woodcock, C. E., 1996, "An Assessment of Several Linear Change Detection Techniques for Mapping Forest Mortality Using Multitemporal Landsat Data," *Remote Sensing of Environment*, 56(1):66-77.

Coppin, P., Jonckheere, I., Nackaerts K., Muys, B., and E. Lambin, 2004, "Digital Change Detection Methods in Ecosystem Monitoring: A Review," *International Journal of Remote Sensing*, 25(9):1565-1596.

Crist, E. P., Laurin, R., and R. C. Cicone, 1986, "Vegetation and Soils Information Contained in Transformed Thematic Mapper Data," in *Proceedings of IGARSS '86 Symposium*, 1465-1470.

Day, E., 1997, *The Southern Pine Beetle Factsheet*, Richmond, VA, Virginia Cooperative Extension, Entomology Publication 444-243.

DBNF (Daniel Boone National Forest), 1999, *Plant Species of the Daniel Boone National Forest* [http://www.fs.fed.us/r8/boone/plants.htm].

de Colstoun, E. C. B., Story, M. H., Thompson, C., Commisso, K., Smith, T. G., and J. R. Irons, 2003, "National Park Vegetation Mapping Using Multitemporal Landsat 7 Data and a Decision Tree Classifier," *Remote Sensing of Environment*, 85(3):316-327.

DeFries, R., Hansen, M., Townshend, J. R. G., and R. Sohlberg, 1998, "Global Land Cover Classifications at 8 km Spatial Resolution: The Use of Training Data Derived From Landsat Imagery in Decision Tree Classifiers" *International Journal of Remote Sensing*, 19(16):3141-3168.

Eastman, R. J., and M. Fulk, 1993, "Long Sequence Time Series Evaluation Using Standardized Principal Components," *Photogrammetric Engineering & Remote Sensing*, 59(8):1307-1312.

Eklund, L. and A. Singh, 1993, "A comparative Analysis of Standardized and Unstandardized Principal Component Analysis in Remote Sensing," *International Journal of Remote Sensing*, 14(7):1359-1370.

Ekstrand, S., 1996, "Landsat TM Based Forest Damage Assessment Correction for Topographic Effects," *Photogrammetric Engineering & Remote Sensing*, 62(2):151-161.

Falkenstrom, H. and S. Ekstrand, 2002, "Evaluation of IRS-1c LISS-3 Satellite Data for Defoliation Assessment on Norway Spruce and Scots Pine," *Remote Sensing of Environment*, 82(1-2):208-223.

Foody, G. M., 2001, "Monitoring the Magnitude of Land-Cover Change Around the Southern Limits of the Sahara," *Photogrammetric Engineering & Remote Sensing*, 67(7):841-847.

Friedl, M. A., Brodley, C. E., and A. Strahler, 1999, "Maximizing Land Cover Classification Accuracies Produced by Decision Trees at Continental to Global Scales," *IEEE Transactions on Geosciences and Remote Sensing*, 37(2):969-977.

Friedl, M. A. and C. E. Brodley, 1997, "Decision Tree Classification of Land Cover from Remotely Sensed Data," *Remote Sensing of Environment*, 61(3):399-409.

Fung, T., 1990, "An Assessment of TM Imagery for Land Cover Change Detection," *IEEE Transactions on Geosciences and Remote Sensing*, 28(4):681-684.

Fung, T. and E. LeDrew, 1987, "Application of Principal Components Analysis for Change Detection," *Photogrammetric Engineering & Remote Sensing*, 53(12):1649-1658.

Goward, S. N., Tucker, C. J., and D. G., Dye, 1985, "North American Vegetation Patterns Observed with the NOAA-7 Advanced Very High Resolution Radiometer," *Vegetatio*, 64(1):3-14.

Hansen, M., Dubayah, R., and R. DeFries, 1996, "Classification Trees: An Alternative to Traditional Land Cover Classifiers," *International Journal of Remote Sensing*, 17(5):1075-1081.

Hansen, M., DeFries R., Townshend, J. R. G., and R. Solberg, 2000, "Global Land Cover Classifications at 1 km Spatial Resolution Using a Classification Tree Approach," *International Journal of Remote Sensing*, 21(6-7):1331-1364.

Herold, N. D., Koeln, G., and D. Cunningham, 2003, "Mapping Impervious Surfaces and Forest Canopy Using Classification and Regression Tree (CART) Analysis," in *ASPRS 2003 Annual Conference Proceedings*, Bethesda, Maryland: American Society for Photogrammetry and Remote Sensing, CD-ROM.

Hodgson, M. E., Jensen, J. R., Tullis, J. A., Riordan, K. D., and C. M. Archer, 2003, "Synergistic Use of Lidar and Color Aerial Photography for Mapping Urban Parcel Imperviousness," *Photogrammetric Engineering & Remote Sensing*, 69(9): 973-980.

Howarth, J. P. and G. M. Wickware, 1981, "Procedure for Change Detection Using Landsat Digital Data," *International Journal of Remote Sensing*, 2(3):277-291.

Huang, C., Davis, L. S., and J. R. G. Townshend, 2002a, "An Assessment of Support Vector Machines for Land Cover Classification," *International Journal of Remote Sensing*, 23(4):725-749.

Huang, C. and J. R. G. Townshend, 2003, "A Stepwise Regression Tree for Non-Linear Approximation: Applications to Estimating Sub-Pixel Land Cover," *International Journal of Remote Sensing*, 24(1):75-90.

Huang, C., Wylie, B., Yang, L., Homer, C., and G. Zylstra, 2002b, "Derivation of a Tasselled Cap Transformation Based on Landsat 7 At-Satellite Reflectance," *International Journal of Remote Sensing*, 23(8):1741-1748.

Huang, C., Zhang, Z., Yang, L., Wylie, B., and C. Homer, 2002c, *MRLC 2001 Image Preprocessing Procedure*, USGS White Paper [http://landcover.usgs.gov/pdf/image_preprocessing.pdf].

Huete, A. R., Justice, C., and H. Liu, 1994, "Development of Vegetation and Soil Indices for MODIS-EOS," *Remote Sensing of Environment*, 49(3):224-234.

Huete, A. R., Liu, H. Q., Batchily, K., and W. van Leeuwen, 1997, "A Comparison of Vegetation Indices Over a Global Set of TM Images for EOS-MODIS," *Remote Sensing of Environment*, 59(3):440-451.

Hutchinson, C. F., 1982, "Techniques for Combining Landsat and Ancillary Data for Digital Classification Improvement," *Photogrammetric Engineering & Remote Sensing*, 48(1):123-130.

Jensen, J. R., 1983, "Biophysical Remote Sensing," *Annals of the Association of American Geographers*, 73(1):111-132.

Jensen, J. R., 1996, *Introductory Digital Image Processing: A Remote Sensing Perspective*, Upper Saddle River, NJ: Prentice-Hall, 318 p.

Jensen, J. R., Ramsey, E. W., Mackey, H. E., Christensen, E. J., and R. P. Sharitz, 1987, "Inland Wetland Change Detection Using Aircraft MSS Data," *Photogrammetric Engineering & Remote Sensing*, 53(5):521-529.

Jha, C. S. and N. V. M. Unni, 1994, "Digital Change Detection of Forest Conversion of Dry Tropical Forest Region," *International Journal of Remote Sensing*, 15(13):2543-2552.

Jordan, C. F., 1969, "Derivation of Leaf Area Index from Quality of Light on the Forest Floor," *Ecology*, 50(4):663-666.

Kauth, R. J. and G. S. Thomas, 1976, "The Tasseled Cap—A Graphic Description of the Spectral-Temporal Development of Agricultural Crops as Seen by Landsat, LARS," in *Proceedings of the Symposium on Machine Processing of Remotely Sensed Data*, West Lafayette, IN: Purdue University, 4B-41-4B-51.

Kwarteng, A. Y. and P. S. Chavez, 1998, "Change Detection Study of Kuwait City and Environs Using Multitemporal Landsat Thematic Mapper Data," *International Journal of Remote Sensing*, 19(9):1651-1661.

Lambert, N. J., Ardo, J., Rock, B. N., and J. E. Vogelmann, 1995, "Spectral Characterization and Regression-Based Classification of Forest Damage in Norway Spruce Stands in the Czech Republic Using Landsat Thematic Mapper Data," *International Journal of Remote Sensing*, 16(7):1261-1287.

Lawrence, R. L. and A. Wright, 2001, "Rule-Based Classification Systems Using Classification and Regression Tree (CART) Analysis," *Photogrammetric Engineering & Remote Sensing*, 67(10):1137-1142.

Liu, H. Q. and A. R. Huete, 1995, "A Feedback Based Modification of NDVI to Minimize Canopy Background and Atmospheric Noise," *IEEE Transactions on Geosciences and Remote Sensing*, 33(2):457-465.

Mas, J. F., 1999, "Monitoring Land-Cover Changes: A Comparison of Change Detection Techniques," *International Journal of Remote Sensing*, 20(1):139-152.

McDonald, E. R., Wu, X., Caccetta, P., and N. Campbell, 2002, *Ilumination Correction of Landsat TM Data in South East NSW*, Canberra, Australia, Department of the Environment and Heritage.

McNab, W. H., 1993, "A Topographic Index to Quantify the Effect of Mesoscale Landform on Site Productivity," *Canadian Journal of Forest Research*, 23(11):1100-1107.

Meyer, P., Itten, K., Kellenberger, T., Sandmeier, S., and R. Sandmeier, 1993, "Radiometric Corrections of Topographically Induced Effects on Landsat TM Data in an Alpine Environment," *ISPRS Journal of Photogrammetry and Remote Sensing*, 48(4):17-28.

Moran, M. S., Jackson, R. D., Slater, P. N., and P. M. Teillet, 1992, "Evaluation of Simplified Procedures for Retrieval of Land Surface Reflectance Factors from Satellite Sensor Output," *Remote Sensing of Environment*, 41(2-3):169-184.

Muchoney, D. M. and B. M. Haack, 1994, "Change Detection for Monitoring Forest Defoliation," *Photogrammetric Engineering & Remote Sensing*, 60(10):1243-1251.

Myneni, R. B., Keeling, C. D., Tucker, C. J., Asrar, G., and R. R. Nemani, 1997, "Increased Plant Growth in Northern Latitudes from 1991 to 1991," *Nature*, 386(6626):698-702.

Nelson, R. F., 1983, "Detecting Forest Canopy Change Due to Insect Activity Using Landsat MSS," *Photogrammetric Engineering & Remote Sensing*, 49(9):1303-1314.

Prakash, A. and R. P. Gupta, 1998, "Land-Use Mapping and Change Detection in a Coal Mining Area—A Case Study in the Jharia Coalfield, India," *International Journal of Remote Sensing*, 19(3):391-410.

Price, T. S., Doggert, H. C., Pye, J. M., and B. Smith, 1998, *A History of Southern Pine Beetle Outbreaks in Southeastern United States*, Macon, GA: Georgia Forestry Commission.

Quinlan, R. J., 1993, *Programs for Machine Learning*, San Mateo, CA: Morgan Kaufman, 302 p.

Riordan, C. J., 1981, "Change Detection for Resource Inventories Using Digital Remote Sensing Data," in *Proceedings of the Workshop on In-Place Resource Inventories: Principles and Practices, University of Maine, Orono, ME, USA*, Bethesda, MD: SAF, 278-283.

Roberts, D. A., Gardner, M., Church, R., Ustin, S., Scheer, G., and R. O. Green, 1998, "Mapping Chaparral in the Santa Monica Mountains Using Multiple End-Member Spectral Mixture Models," *Remote Sensing of Environment*, 65(3):267-279.

Rogan, J., Franklin, J., and D. A. Roberts, 2002, "A Comparison of Methods for Monitoring Multitemporal Vegetation Change Using Thematic Mapper Imagery," *Remote Sensing of Environment*, 80(1):143-156.

Royle, D. D. and R. G. Lathrop, 1997, "Monitoring Hemlock Forest Health in New Jersey Using Landsat TM Data and Change Detection Techniques," *Forest Science*, 43(3):327-335.

RuleQuest Research, 2001, *See5 Data Mining Software, Version 1.13*, St. Ives, NSW, Australia, RuleQuest Research.

Sabins, F. F., 1987, *Remote Sensing: Principles and Interpretation*, New York, NY: W. H. Freeman and Company, 449 p.

ingh, A., 1989, "Digital Change Detection Techniques Using Remotely-Sensed Data," *International Journal of Remote Sensing*, 10(6):989-1003.

Seto, K. C., Woodcock, C. E., Song, C., Huang, X., Lu, J., and R. K. Kaufmann, 2002, "Monitoring Land Use Change in the Pearl River Delta Using Landsat TM," *International Journal of Remote Sensing*, 23(10):1985-2004.S

Singh, A. and A. Harrison, 1985, "Standardized Principal Components," *International Journal of Remote Sensing*, 6(6):883-896.

Skakun, R. S., Wulder, M. A., and S. E. Franklin, 2003, "Sensitivity of the Thematic Mapper Enhanced Wetness Difference Index to Detect Mountain Pine Beetle Red-Attack Damage," *Remote Sensing of Environment*, 86(4):433-443.

Smith, J. A., Lin, T. L., and K. J. Ranson, 1980, "The Lambertian Assumption and Landsat Data," *Photogrammetric Engineering & Remote Sensing*, 46(9):1183-1189.

Sohl, T., 1999, "Change Analysis in the United Arab Emirates: An Investigation of Techniques," *Photogrammetric Engineering & Remote Sensing*, 65(4):475-484.

Strahler, A., Logan, T. L., and N. A. Bryant, 1978, "Improving Forest Classification Accuracy from Landsat by Incorporating Topographic Data," in *Proceedings of the Twelfth International Symposium on Remote Sensing of Environment*, Ann Arbor, Michigan, 927-942.

Teillet, P. M., Guindon, B., and D. G. Goodenough, 1982, "On the Slope-Aspect Correction of Multispectral Scanner Data," *Canadian Journal of Remote Sensing*, 8(2):84-106.

Tou, J. T. and R. C. Gonzalez, 1974, *Pattern Recognition Principles*, Reading, MA: Addison-Wesley Publishing Company, 377 p.

Townshend, J. R. G. and C. O. Justice, 1995, "Spatial Variability of Images and the Monitoring of Changes in the Normalized Difference Vegetation Index," *International Journal of Remote Sensing*, 16(12):2187-2195.

Townshend, J. R. G., Justice C. O., Skole, D., Malingreau, J. P., Cihlar J., Teillet, P., Sadowski, F., and S. Ruttenberg, 1994, "The 1 km Resolution Global Data Set: Needs of the International Geosphere Biosphere Program," *International Journal of Remote Sensing* 15(17):3417-3442.

Vogelmann, J. E., Helder, D., Morfitt, R., Choate, M. J., Merchant, J. W. and H. Bulley, 2001, "Effects of Landsat 5 Thematic Mapper and Landsat 7 Enhanced Thematic Mapper Plus Radiometric and Geometric Calibrations and Corrections on Landscape Characterization," *Remote Sensing of Environment*, 78(1-2):55-70.

Vogelmann, J. E. and B. N. Rock, 1989, "Use of Thematic Mapper Data for the Detection of Forest Damage Caused by the Pear Thrips," *Remote Sensing of Environment*, 30(3):217-225.

Weismiller, R. A., Kristof, S. J., Scholz, D. K., Anuta, P. E., and S. A. Momin, 1977, "Change Detection in Coastal Zone Environments," *Photogrammetric Engineering & Remote Sensing*, 43(12):1533-1539.

Williams, D. L. and R. F. Nelson, 1986, "Use of Remotely Sensed Data for Assessing Forest Stand Condition in the Eastern United States," *IEEE Transactions on Geosciences and Remote Sensing*, 24(1): 130-138.